

Title : will be set by the publisher
Editors : will be set by the publisher
EAS Publications Series, Vol. ?, 2018

GAS DYNAMICS IN CENTRAL PARTS OF GALAXIES

Witold Maciejewski¹

Abstract. Asymmetries in galactic potentials, either self-induced, or caused by a passing companion, play an important role in global gas dynamics in galaxies. In particular, they are able to trigger gas inflow, which in turn feeds nuclear activity. In the inner kiloparsec, the inflowing gas becomes subject to various resonances induced by asymmetry in the potential. This produces complicated gas morphology and dynamics seen in the nuclear rings and spirals. Formation of nuclear rings is related to barred galaxies, and explained by the orbital structure in bars. One can get basic understanding of weak nuclear spirals from the linear wave theory, but stronger spirals are likely to be out of the linear regime, and they appear as spiral shocks in hydrodynamical models. In addition, nuclear stellar bars are observed in a considerable fraction of disc galaxies, often nested inside the large bar; their orbital structure further modifies the nuclear gas dynamics. If a massive black hole (MBH) is present in the galactic centre, it governs the resonances even beyond its classically defined sphere of influence. Since resonances shape gas dynamics in the nuclear region, the central black hole should be able to regulate gas flow around itself.

1 Introduction

Nuclear starbursts and Active Galactic Nuclei (AGN) have to be fed by mass transport into the active regions. Due to dissipation, gas inflow is easiest to trigger. There are two obvious dynamical mechanisms causing gas inflow in galaxies: interactions and asymmetries in galactic potentials. The first one involves violent and transient phenomena with strong gas inflow towards the centres of the interacting galaxies seen in numerical simulations (see e.g. Mihos & Hernquist 1996). Closer analysis of the modeled merging sequence shows that the inflow process has two stages: first, tidal perturbations destabilize stellar discs, and then, each disturbed stellar disc exerts torques on the gas, and triggers inflow. Thus even in

¹ INAF – Osservatorio Astrofisico di Arcetri, Largo E. Fermi 5, 50125 Firenze, Italy,
 and Obserwatorium Astronomiczne Uniwersytetu Jagiellońskiego, Cracow, Poland

systems apparently as order-less as merging galaxies, gas dynamics is governed by the perturbed potentials of each individual galaxy.

Here I review the dependence of gas dynamics on the gravitational potential in isolated galaxies, where it can be seen more clearly, since these galaxies remain roughly unchanged on timescales corresponding to the formation of steady gas flow patterns. Inflow in isolated galaxies can occur steadily, which may in principle provide continuous feeding of the central activity. However, the presence and the positions of dynamical resonances determine the mode of gas flow in the nuclear region: it may be quite complex, as the recent high-resolution observations of galactic centres indicate. Structured dust lanes, nested bars, as well as nuclear rings and spirals have been observed (Regan & Mulchaey 1999, Martini & Pogge 1999, Pogge & Martini 2002, Erwin & Sparke 2002).

First, I briefly review global gas flow patterns in the most common asymmetry in disc galaxies, i.e. in the presence of a stellar bar (§2), and then, in subsections of §3, I explore various modes of gas flow in the nuclear region. I also attempt to determine which modes may trigger significant inflow capable of feeding the AGN. Placing a Massive Black Hole (MBH) at the galaxy centre may add, remove or shift resonances, therefore such a black hole may regulate gas flow around itself. Finally, I make a few remarks on numerical methods (§4).

2 Gas dynamics in a barred galaxy outside the nuclear ring

Galactic discs commonly develop stellar bars, and the majority of observed galaxies is barred (e.g. Eskridge et al. 2000). The most established observational notion about gas morphology in barred galaxies is the existence of two straight or curved dust lanes in the main body of the stellar bar, which are symmetric around the galaxy centre, and slightly tilted to the bar's major axis (see e.g. NGC 1097, NGC 1300, NGC 4303, and NGC 6951 in the Hubble Atlas of Galaxies, Sandage 1961). Strong discontinuities in gas velocity, indicative of shocks, have been measured along the dust lanes (Regan et al. 1997). This morphology and kinematics have been seen in numerical models of gas flow in a fixed potential of the bar since the work of Sørensen et al. (1976). It has been explained in terms of stable periodic orbits by Athanassoula (1992).

There are two major families of stable prograde periodic orbits inside the bar: the x_1 orbits parallel to the bar, and the x_2 orbits orthogonal to it (Contopoulos & Papayannopoulos 1980). The x_2 orbits are present only in galaxies with sufficient central mass concentrations and moderate bar pattern speeds — in linear analysis this condition corresponds to the existence of an Inner Lindblad Resonance (ILR, see Binney & Tremaine 1987, and §3). By definition, the x_2 orbits exist only inside this resonance. Representative orbits of each family are plotted in Figure 1.

In the outer parts of the bar, gas tends to follow the x_1 orbits. Further inwards, the x_1 orbits develop cusps and loops: stars can follow such orbits, but gas on self-intersecting orbits gets shocked. A robust feature in the majority of numerical models is a pair of principal shocks that develop on the leading side of the bar (marked PS in Fig.1). There, torques transfer angular momentum from

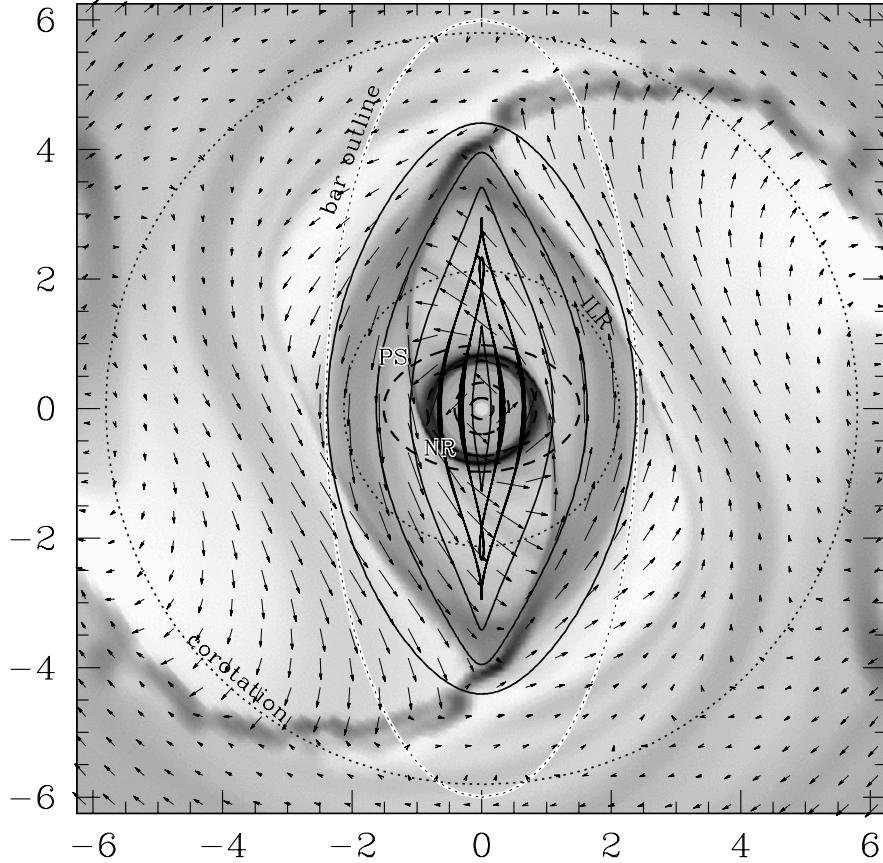


Fig. 1. A representative snapshot of the gas density and velocity field in a barred galaxy, taken after 6 rotation periods of the bar, once the main flow patterns have been established. The gas, treated as a non-selfgravitating, isothermal fluid with a sound speed of 5 km/s, responds to a fixed gravitational potential of a bar, disc and spheroid, and is modeled with an Eulerian code on a fixed grid. The density is shown in grayscale, and arrows mark gas velocity in the reference frame rotating with the bar. Dotted circles mark corotation and the ILR. Examples of x_1 and x_2 orbits are drawn with solid and dashed lines, respectively. **PS** marks the principal shock in the bar, **NR** is the nuclear ring. Units on axes are in kpc. From the model S05 by Maciejewski et al. (2002)

the gas to the bar, and the gas falls towards the centre. Numerical models indicate considerable gas inflow in the principal shocks: up to $1 \text{ M}_\odot \text{ yr}^{-1}$ for typical gas densities in the disc (Athanasoula 1992; Regan et al. 1997). The shocked gas usually does not flow straight to the galaxy centre: it tends to settle on the x_2 orbits, which have lower value of the Jacobi integral E_J (corresponding to the energy in the rotating frame). Consequently, the straight shocks are slightly tilted to the bar's major axis. If there were no x_2 orbits, straight shocks would develop

on the bar's major axis, possibly extending directly to the centre of the galaxy (Athanasoula 1992, Piner et al. 1995). Only a couple of galaxies with such central (on-axis) straight shocks have been observed (Athanasoula 1992), which suggests that most barred galaxies possess the ILR. The gas settling on x_2 orbits, well inside the ILR (see Fig.1), often accumulates in nuclear rings, where high density and no shear make favorable conditions for star formation (Piner et al. 1995). Star-forming nuclear rings have been observed in many galaxies (e.g. NGC 1512, Maoz et al. 2001; NGC 4314, Benedict et al. 2002). Nuclear rings may also form in a potential lacking an ILR, given that this potential is almost axisymmetric at the nucleus (Wada, priv. comm.).

3 Gas dynamics around resonances inside the nuclear ring

At resonances, the orbital frequency (Doppler-shifted to the reference frame of the bar) is commensurate with the frequency of radial oscillations. Thus a particle (or a gas cloud) at the resonance is subject to a monotonic force, which moves it away from there. The influence of the ILR is the strongest: it creates the principal shocks described in §2. For a bar rotating with a pattern speed Ω_B , the ILR occurs where the orbital frequency Ω and the frequency of radial oscillations κ are related by $\Omega - \Omega_B = \kappa/2$. Since $\Omega_B = \text{const}$, it is convenient to rewrite this condition as $\Omega - \kappa/2 = \Omega_B$, where $\Omega - \kappa/2$ is called the frequency curve.

3.1 The Triple ILR scenario

The frequency curve always declines towards zero at large radii. It goes to $+\infty$ at the galactic centre if a central MBH is present, but even without a central MBH it can reach high values (larger than Ω_B) at the nucleus, if the galaxy mass is sufficiently centrally concentrated. Thus, in such galaxies one should expect at least one ILR. However, if a galaxy has a central MBH, but a low central mass concentration otherwise, the resonance curve may not be monotonic, and 3 ILRs can occur (Fig.2). They are called (from the innermost out) the nuclear ILR, the inner ILR and the outer ILR.

The nuclear ILR is essentially related to the presence of the central MBH. Fukuda et al. (1998, 2000) showed that gas flow around this resonance closely resembles the flow around the outer ILR described in §2. This gas morphology may prove essential in finding central MBHs in galaxies: as can be seen in Figure 2, the nuclear ILR is located at the radius a few times larger than the MBH's radius of influence (minimum of the rotation curve). Therefore we can learn about the central MBH from the gas morphology at radii larger than the ones useful in the conventional methods of stellar kinematics. On the other hand, shocks around the nuclear ILR strongly disturb gas kinematics; in this case, the assumption of a circularly rotating disc, common when MBH mass is derived from kinematics of ionized gas (e.g. Macchetto et al. 1997), may no longer be valid.

Because of the small size of the ring inside the nuclear ILR, the gas accumulating there may reach very high densities, so that self-gravity in gas will be

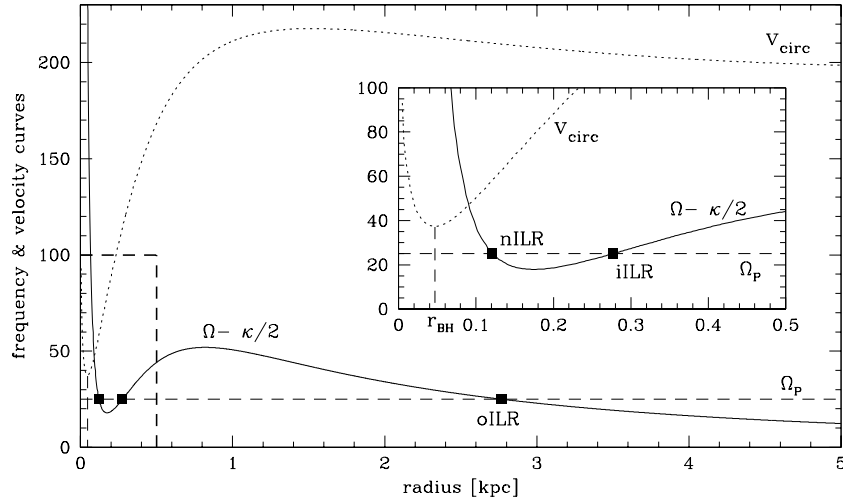


Fig. 2. Velocity and frequency curves for a potential with 3 ILRs. The circular velocity (v_{circ}) is drawn with dotted line, the frequency curve is solid. The constant pattern speed Ω_P is marked with the horizontal dashed line. Positions of the three ILRs: nuclear (nILR), inner (iILR), and outer (oILR) are marked with squares. A close-up of the inner region is shown in the insert, where the sphere of influence of the $10^7 M_\odot$ MBH has roughly the radius r_{BH} .

the dominating force. Fukuda et al. (2000) investigated the evolution of such a self-gravitating ring, and showed that strong inflow induced by clumps in self-gravitating gas will occur. This is one of the viable mechanisms of feeding the AGN; here the central MBH enhances inflow onto itself due to the resonance that it generates. Another possible scenario involves efficient star formation in the ring, which leads to a nuclear starburst driven by the MBH.

Gas dynamics at the inner ILR is considerably different from that at the nuclear ILR and at the outer ILR. The orbital transition is different there as well: at the outer ILR, gas moves from the x_1 orbits with higher Jacobi integral E_J to the nearly-circular x_2 ones with lower E_J . Inside the inner ILR, gas has to populate the x_1 orbits, which may be highly elongated at the centre (see Fig.1). The transition from the flow along the x_2 orbits to the one following the x_1 family creates a *leading* spiral at the inner ILR (Wada 1994, Knapen et al. 1995). The dynamics of this spiral is markedly different from the trailing spirals that form at the nuclear and outer ILRs: it reflects a converging flow rather than a shock, with the hot gas upstream from the arm (Wada & Koda 2001).

3.2 Central rotation curves and mass profiles in galactic centres

The triple ILR scenario predicts reversal of the spiral structure in the central parts of galaxies. Going inwards from the trailing spiral arms and the principal shocks

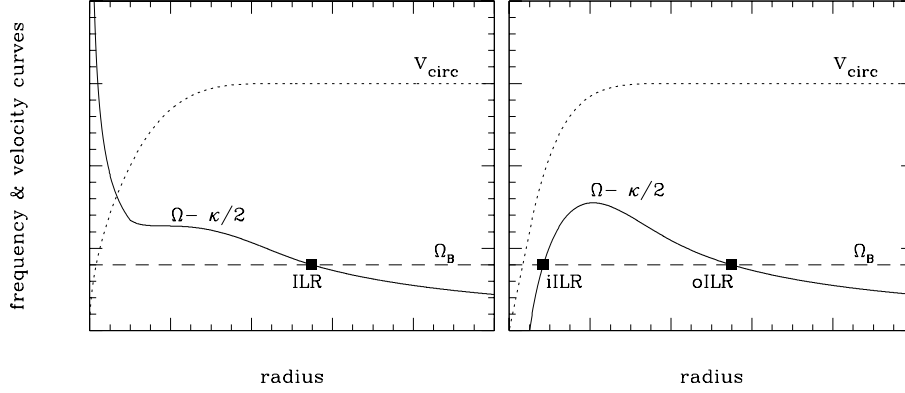


Fig. 3. Two sample rotation curves (dotted): both are flat at large radii, but the one on the left shows power-law rise at the centre, while the one on the right rises linearly. Solid line marks the corresponding frequency curves with positions of resonances (marked as in Fig.2) for a given pattern speed Ω_B .

in the bar, one should encounter the leading spiral at the inner ILR, and then a trailing one again in the innermost regions. This is not a commonly observed structure (§3.3), which undermines the viability of the frequency curve in Figure 2. Furthermore, fits to surface brightness profiles of disc galaxy nuclei show a very good agreement with power-law profile (Balcells et al. 2001). For a power-law luminosity profile, the rotation curve is also a power law (with positive exponent), as is the frequency curve (negative exponent here), which means that the latter rises monotonously inwards, and therefore has one ILR only.

The frequency curve is a derivative of the rotation curve, and is therefore more sensitive to the variation of the rotation curve's shape than to its value. Consider two rotation curves (Fig.3), both flat at large radii, but one a power-law in the inner part, while the other one has a linear inner rise. Although they both may fit a given set of observed data equally well, they generate diametrically different frequency curves. The rotation curve with an inner power-law results in an inner power-law frequency curve, which rises monotonically inwards (innermost radii in left panel of Fig.3). This implies one ILR only. On the other hand, a linearly rising rotation curve indicates solid body rotation, for which the frequency curve is identically equal to zero (innermost radii in right panel of Fig.3). This forces an additional ILR on the system, and now both outer ILR and inner ILR are present. Therefore, a linear rise of the central rotation curve, although a good approximation to the data, may not properly reflect the mass distribution in the inner parts of galaxies, or the resonances that it induces. Special care has to be taken when the presence and the position of resonances are deduced from the observed rotation curve. Resolution effects, like beam smearing, give the impression of a linear rise in the central parts, which unavoidably implies the presence of an inner ILR.

3.3 Gas density waves within a single ILR

Recent high-resolution maps of galactic centres reveal intricate dust structures, which are often organized in a spiral pattern (Regan & Mulchaey 1999, Pogge & Martini 2002). In disc galaxies, these *nuclear spirals*, often winding by more than a 2π angle, seem to connect smoothly to the outer spiral arms or to the principal dust lanes in the bar. This makes an indirect argument against the presence of an inner ILR, since theory and modeling indicate the reversal of the spiral there (§3.1). On the other hand, the standard model of gas flow in the bar (§2) does not account for nuclear spirals either: gas settles there in the nuclear ring. Models by Athanassoula (1992) show curling of the inner parts of the principal shock, but the resolution is too low there to follow this feature further inwards.

For a given potential, gas flow depends sensitively on one parameter only: the velocity dispersion in the gas, which for an isothermal gas is represented by its temperature (Englmaier & Gerhard 1997; Patsis & Athanassoula 2000). Gas dynamics in the nuclear region changes remarkably with the sound speed in the isothermal gas (c_S): cold gas ($c_S \sim 5$ km/s) settles on the nuclear ring, as described in §2, while hot gas ($c_S > 10$ km/s) forms a nuclear spiral (Maciejewski 1998). In the evolutionary sequence of gas flow in the bar, the principal shocks form first as trailing spirals, and then straighten as the bar grows in strength, with their inner parts curling inwards (Fig.4). In hot gas, the curling shock from one side of the bar never meets its counterpart from the opposite side, and both of them propagate towards the centre as an $m=2$ spiral mode. The convergence of the flow in such created nuclear spiral is high (large negative $\text{div}\mathbf{v}$), which is indicative of a shock.

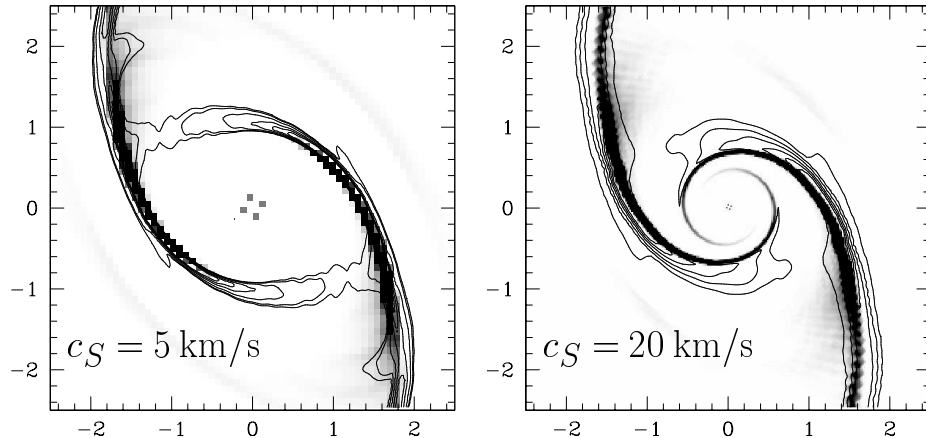


Fig. 4. *Left:* A snapshot of gas flow with density marked by contours, and $\text{div}^2\mathbf{v}$ for $\text{div}\mathbf{v} < 0$ (shock indicator) in grayscale for model S05 of cold gas from Maciejewski et al. (2002) at 0.1 Gyr, when gas leaving one principal shock reaches the opposite one. *Right:* A snapshot at the same time for model S20 of hot gas. Contours are at 1.7 (1.4 right), 2, 3, 5, 7 and 9 times the initial gas density. Units on axes are in kpc.

Significant gas inflow to the galactic centre may occur if the spiral shock proves to be efficient in transferring angular momentum from the gas to the bar. On the other hand, the principal shock in cold gas ceases to propagate inwards. Gas emerging from its innermost parts remains on a relatively open trajectory (Fig.4), and hits the shock on the opposite side of the bar. Hydrodynamical interaction of the flow with the shock results here in gas settling into the nuclear ring.

A good grasp of the dynamics of nuclear spirals can be gained when one considers them as density waves generated by gravitational torques in a non-selfgravitating gas (Englmaier & Shlosman 2000). In the linear approximation, the dispersion relation for the $m=2$ mode allows for wave propagation inside the corotation only when $\Omega - \kappa/2 > \Omega_B$, i.e. between the outer ILR and the inner ILR (if present) or the galactic centre. Since nuclear spirals are observed in disc galaxies down to the HST resolution limit, the inner ILR must reside inside that radius in these galaxies, if it is present at all.

Although some nuclear spirals in strongly barred galaxies may be well out of the linear regime, the density-wave mechanism applies to a weak spiral inside the nuclear ring seen in the models by Maciejewski et al. (2002). It is also extremely efficient in very weak bars, where gas dynamics closely follows the linear theory. Its predictions are the same for any weak nonaxisymmetry of the potential, including lopsidedness, because low harmonics of the mass distribution play a role there. Maciejewski (2001) studied gas flow in the gravitational potential with the quadrupole moment of the bar 10 times lower, and the bar's axis ratio half that of the standard model presented in §2. Such a bar is likely to be too weak to be detected observationally, and it does not generate principal shocks of any shape. Nevertheless, a clear spiral density enhancement is seen inside the ILR. In accordance with the density-wave theory, it extends all the way to the galactic centre if there is no inner ILR, or ceases at the inner ILR if it is present. Unlike nuclear spirals in strong bars, which unwind outwards rapidly in order to match the principal shock in the bar, nuclear spirals in very weak bars follow the linear mode longer, and wind up to 3 times around the centre (6π angle). Thus tightly wound nuclear spirals may be observationally associated with galaxies where no bar has been detected.

3.4 *Sorting out distinct scenarios of gas flow in nested bars*

Galaxies possessing nested bars (a secondary bar inside the main one) have been noticed already almost 30 years ago (de Vaucouleurs 1974), but only recent studies (Laine et al. 2002, Erwin & Sparke 2002) showed them to be quite a common phenomenon: up to 30% of barred galaxies contain nested stellar bars. The random relative orientation of the bars suggests that they rotate independently. For a while nested bars became a favourite mechanism to fuel the nucleus: if gas flow in the secondary bar is analogous to the one in the main bar, then the secondary bar may force gas deeper into the potential well. Meanwhile, the pioneering work of Shlosman et al. (1989) examined fueling mechanism that involves instability in the self-gravitating nuclear gaseous disc. As the gas inflow in the large bar stagnates

at the nuclear ring or disc, gas accumulates there, and can become gravitationally unstable. By analogy to instability of the galactic stellar disc, Shlosman et al. proposed that a *gaseous* inner bar forms inside the large bar (gaseous bar scenario).

The gaseous bar scenario may be related to the observed nested *stellar* bars, when star formation occurs in the dense gaseous inner bar, or when the inner gaseous bar drags stars of the nuclear component (Combes 1994). Neither of these links is likely though, since the gaseous bar scenario relies on *global* instability in self-gravitating gas, while cold massive nuclear discs are more likely to become unstable *locally*, and form clumps. This is clearly seen in simulations by Heller & Shlosman (1994): although the nuclear gaseous disc first collapses into a bar-like shape, clumps develop very quickly, so that no bar is seen a few Myr after its formation. This time is too short to form stars or to alter stellar dynamics, and the star-forming clumps do not follow bar-like orbits either. Therefore nested *stellar* bars are unlikely to be produced by the gaseous bar scenario. However, this scenario may lead to an episodic gas inflow: one galaxy where it may operate is Circinus (Maiolino et al. 2000) — one of the three closest AGN. A strong gas inflow on a scale ~ 50 pc is seen on one side of the nucleus, but it is not accompanied by any outflow. It is likely that the unstable gaseous disc developed an $m = 1$ instability mode there, and is feeding the nucleus in a short episode.

In order to estimate the dynamical significance of the gaseous component Friedli & Martinet (1993) and Combes (1994) looked for formation of nested bars in numerical simulations involving stellar and gaseous particles. They were able to create secondary *stellar* bars, which decouple from the large bars after the central mass concentration increases substantially as a result of gas inflow in the large bar. These inner stellar bars can then drag gas with them. In this mechanism, the role of gas is to increase central mass concentration, and to prevent heating of the central stellar component. No gravitational instability in the gaseous disc is involved, contrary to the mechanism proposed by Shlosman et al. (1989). Note however that these simulations use numerical methods suffering from excessive gas inflow to the centre (see §4), and therefore central mass concentrations may be unrealistically high, which undermines their conclusion. Also, the size ratio of the bars produced in this mechanism (Set III in Friedli & Martinet 1993) is 2 — much lower than the observed values. It indicates that these models may miss the physical mechanisms operating in the observed systems. A more realistic size ratio (3.8) is produced in Set II of Friedli & Martinet, but there the gas only prevents stars from heating, and the initial conditions are particularly chosen so that two bars are formed.

Since inner bars are often observed in near infrared, they are most likely made out of old stellar populations, and are long-lived. They are often devoid of gas, hence it is likely that purely stellar-dynamical mechanisms forming decoupled nested bars are in operation there (Rautiainen & Salo 1999). Maciejewski & Sparke (2000) explored limitations which are imposed on nested stellar bars by their orbital structure. Since orbits in a potential of two independently rotating bars (a class of pulsating potentials) do not close in general, they generalized the concept of the orbit to pulsating potentials, and found sets of particles populating

closed curves that support bars in their motion. If resonant coupling is assumed to minimize the number of chaotic zones (Sygnet et al. 1988), then curves hosting sets of particles that support the inner bar are round and end well within its corotation, so that no shocks in gas are induced. Maciejewski et al. (2002) confirmed this with hydrodynamical simulations: gas flow in the inner stellar bar, which is in resonant coupling with the large bar, does not develop straight shocks, and does not increase the inflow. It instead organizes itself in an ellipsoidal pattern around the inner bar, like the one seen in color maps of NGC 3081 (Regan & Mulchaey 1999). Nevertheless, nested bars may not follow the resonant coupling assumed in this scenario, and other modes of gas flow in the inner bar are possible, including straight dust lanes (Maciejewski 2002).

4 Remarks about numerical methods

Numerical methods used in modeling of gas flow in galaxies can generally be divided into 3 classes: one treats gas as a set of ballistic clouds with some rules for energy and momentum exchange (sometimes called 'sticky particles'), the second solves hydrodynamical equations involving the SPH algorithm (Smooth Particle Hydrodynamics), while the third solves these equations directly on the grid. The first method, and to some extent the second, involves a number of free parameters in gas description, which can be adjusted to describe particular features of the ISM. On the other hand, the third method may involve algorithms (like the Riemann solver) which limit the set of free parameters to purely numerical ones, and which attempt to give the best approximation to the dynamics of non-viscous gas. This leads to unique hydrodynamical solutions, but it remains unclear how the real ISM differs from non-viscous fluid.

Consequences of numerical viscosity are particularly significant in studies of gas inflow. Bulk viscosity in SPH-based codes is necessary to stabilize post-shock oscillations, and it is quite large. One can compare the evolution of density within the inner 300 pc (inside the nuclear ring) in the grid-based model (Piner et al. 1995) to that in the SPH model (Patsis & Athanassoula 2000) for the same potential: in the first model, the density remains roughly constant, while in the second one it increases by more than a factor of 50 after 8 pattern rotations. Such a central mass concentration may be not realistic, and its strong dynamical influence, postulated by Friedli & Martinet (1993) and others, may not be relevant to present-day galaxies. Also the importance of self-gravity in gas may need to be scaled down. Heller & Shlosman (1994) measure mass of gas within 500 pc at some stage of their SPH simulations to be half of the dynamical mass. This is significantly more than the observed values (see e.g. Sakamoto et al. 1999). They also measure the mass of the central gas clump to be $3 \times 10^9 M_\odot$, when usually no more than $10^9 M_\odot$ of gas is seen in galaxy centres. In the SPH simulations by Berentzen et al. (1998) a considerable amount of gas quickly falls onto the 'central accreting object', so that mass in gas accumulated there amounts to 1.6% of the total galaxy mass. This is an order of magnitude larger than the currently measured central MBH masses (Kormendy & Gebhardt 2001).

All 3 classes of methods discussed above usually represent the ISM as an isothermal fluid. Although this is a valid approximation (Cowie 1980), which has produced many significant results so far, one will eventually need a more realistic description of the ISM. Immense progress has been made here in the recent years by Wada & Norman (1999, 2001), who developed a grid-based code which allows for cooling and heating of the gas, as well as for self-gravity. As a result, a multiphase medium forms, with lognormal density distribution over 4 orders of magnitude. Shear by differential rotation seems to be sufficient to create flocculent nuclear spirals, and dynamics of this medium in presence of a weak bar has been studied recently (Wada & Koda 2001).

5 Conclusions

Asymmetries in the galactic potential can alter gas dynamics, generate inflow, and consequently speed up galaxy evolution. Gas dynamics in centres of galaxies strongly depends on the presence of resonances created by asymmetries in the potential. The presence and the number of resonances is regulated by the central mass distribution. In particular, the MBH in the centre of galaxy can create and/or move the resonances, and thus regulate gas flow around itself. Grand design nuclear spirals observed in centres of galaxies are consistent with the presence of one ILR only. Some of them may be sites of shocks that increase inflow to the galactic centre.

Two fundamentally different gas flows have been labeled as 'gas flow in nested bars', which often causes confusion. One mode of the flow, originally proposed by Shlosman et al. (1989), refers to gaseous inner bars, which form in unstable gaseous nuclear discs. In this scenario the bar *is* the flow: it involves rapid radial gas motion on timescales of the order of dynamical time. It may be able to feed the AGN, but modeling work was not able yet to find connection between it and the nested stellar bars that we observe in galaxies. The second scenario refers to the flow in nested stellar bars. Stable orbits supporting such systems enable their long lifetime, and at the same time they restrict gas flow to follow elliptical trajectories (Maciejewski & Sparke 2000). In this scenario nested bars do not increase inflow to the galactic centre.

Acknowledgments. I would like to thank the organizers of the Galactic Dynamics Workshop at the JENAM 2002 Symposium for their invitation to give this review. Insightful comments by Lia Athanassoula, Eric Emsellem, Peter Erwin, Roberto Maiolino, Alessandro Marconi, Eva Schinnerer, Peter Teuben and Keiichi Wada have been invaluable to this review.

References

- Athanassoula, E. 1992, MNRAS, 259, 345
 Balcells, M., Domínguez-Palmero, L., Graham, A., & Peletier, R. F. 2001, ASP

- Conf. Ser. 249: The Central Kiloparsec of Starbursts and AGN: The La Palma Connection, 167
- Benedict, G. F., Howell, D. A., Jørgensen, I., Kenney, J. D. P., & Smith, B. J. 2002, *AJ*, 123, 1411
- Berentzen, I., Heller, C. H., Shlosman, I., & Fricke, K. J. 1998, *MNRAS*, 300, 49
- Binney, J. & Tremaine, S. 1987, *Galactic Dynamics* (Princeton: Princeton Univ. Press)
- Combes, F. 1994, in *Mass-Transfer Induced Activity in Galaxies* (Cambridge: Cambridge Univ. Press), 170
- Contopoulos, G. & Papayannopoulos, T. 1980, *A&A*, 92, 33
- Cowie, L. L. 1980, *ApJ*, 236, 868
- de Vaucouleurs, G. 1974, *IAU Symp. 58: The Formation and Dynamics of Galaxies*, 335
- Englmaier, P. & Gerhard, O. 1997, *MNRAS*, 287, 57
- Englmaier, P. & Shlosman, I. 2000, *ApJ*, 528, 677
- Erwin, P. & Sparke, L. S. 2002, *AJ*, 124, 65
- Eskridge, P. B. et al. 2000, *AJ*, 119, 536
- Friedli, D. & Martinet, L. 1993, *A&A*, 277, 27
- Fukuda, H., Wada, K., & Habe, A. 1998, *MNRAS*, 295, 463
- Fukuda, H., Habe, A., & Wada, K. 2000, *ApJ*, 529, 109
- Heller, C. H. & Shlosman, I. 1994, *ApJ*, 424, 84
- Knapen, J. H., Beckman, J. E., Heller, C. H., Shlosman, I., & de Jong, R. S. 1995, *ApJ*, 454, 623
- Kormendy, J. & Gebhardt, K. 2001, *20th Texas Symposium on relativistic astrophysics*, 363
- Laine, S., Shlosman, I., Knapen, J. H., & Peletier, R. F. 2002, *ApJ*, 567, 97
- Macchetto, F., Marconi, A., Axon, D. J., Capetti, A., Sparks, W., & Crane, P. 1997, *ApJ*, 489, 579
- Maciejewski, W. 1998, Ph.D. Thesis, Univ. of Wisconsin
- Maciejewski, W. 2001, *ASP Conf. Ser. 249: The Central Kiloparsec of Starbursts and AGN: The La Palma Connection*, 153
- Maciejewski, W. 2002, *ASP Conf. Ser. 275: Disks of Galaxies: Kinematics, Dynamics and Perturbations*, 251
- Maciejewski, W. & Sparke, L. S. 2000, *MNRAS*, 313, 745
- Maciejewski, W., Teuben, P. J., Sparke, L. S., & Stone, J. M. 2002, *MNRAS*, 329, 502
- Maiolino, R., Alonso-Herrero, A., Anders, S., Quillen, A., Rieke, M. J., Rieke, G. H., & Tacconi-Garman, L. E. 2000, *ApJ*, 531, 219
- Maoz, D., Barth, A. J., Ho, L. C., Sternberg, A., & Filippenko, A. V. 2001, *AJ*, 121, 3048
- Martini, P. & Pogge, R. W. 1999, *AJ*, 118, 2646
- Mihos, J. C. & Hernquist, L. 1996, *ApJ*, 464, 641
- Patsis, P. A. & Athanassoula, E. 2000, *A&A*, 358, 45
- Piner, B. G., Stone, J. M., & Teuben, P. J. 1995, *ApJ*, 449, 508
- Pogge, R. W. & Martini, P. 2002, *ApJ*, 569, 624
- Regan, M. W., Vogel, S. N., & Teuben, P. J. 1997, *ApJL*, 482, L143

- Regan, M. W. & Mulchaey, J. S. 1999, *AJ*, 117, 2676
- Rautiainen, P. & Salo, H. 1999, *A&A*, 348, 737
- Sakamoto, K., Okumura, S. K., Ishizuki, S., & Scoville, N. Z. 1999, *ApJ*, 525, 691
- Sandage, A. 1961, *The Hubble Atlas of Galaxies* (Washington: Carnegie Institution)
- Shlosman, I., Frank, J., & Begelman, M. C. 1989, *Nat*, 338, 45
- Sørensen, S.-A., Matsuda, T., & Fujimoto, M. 1976, *Ap&SS*, 43, 491
- Syget, J. F., Tagger, M., Athanassoula, E., & Pellat, R. 1988, *MNRAS*, 232, 733
- Wada, K. 1994, *PASJ*, 46, 165
- Wada, K. & Koda, J. 2001, *PASJ*, 53, 1163
- Wada, K. & Norman, C. A. 1999, *ApJL*, 516, L13
- Wada, K. & Norman, C. A. 2001, *ApJ*, 547, 172